

Citation: Löscher, A., and G. Kirchengast: Assimilation of GNSS Radio Occultation Profiles into GCM Fields for Global Climate Analysis, in: Atmosphere and Climate: Studies by Occultation Methods (U. Foelsche, G. Kirchengast, A.K. Steiner, eds.), Springer, Berlin-Heidelberg, 325-334, 2006.

Assimilation of GNSS Radio Occultation Profiles into GCM Fields for Global Climate Analysis

A. Löscher and G. Kirchengast

Wegener Center for Climate and Global Change (WegCenter) and Institute for Geophysics, Astrophysics, and Meteorology (IGAM), University of Graz, Austria
armin.loescher@uni-graz.at

Abstract. This paper investigates the application of the 3D-Var methodology within a global climate monitoring framework. It studies the assimilation of GNSS radio occultation derived refractivity profiles into ECMWF analysis or short-term forecast fields as background. The system is tuned for high vertical and moderate horizontal resolution, best suited to the spatial characteristics of these satellite based measurements. The analyses are performed on a GCM-compliant Gaussian grid, comprising 60 model levels up to a height of ~60 km and a horizontal resolution corresponding to a triangular spectral truncation T42 (i.e., T42L60). Within the system two different operational modes are implemented, the first updating a refractivity background, derived from ECMWF analysis fields, the second directly updating the ECMWF temperature, specific humidity and surface pressure fields. First results indicate a significant analysis increment, emphasising the ability of RO data to add independent information to ECMWF analysis fields.

1 Introduction

Relatively new measurement concepts like GNSS RO (Global Navigation Satellite System Radio Occultation) offer the opportunity to develop new processing techniques and strategies to exploit the data in the best possible and most efficient way. The RO experiment on-board CHAMP (e.g., Wickert et al. 2004) is the first system, which delivers continuous observations on a quasi-operational basis, preparing the ground for the first RO-only based global climatologies. With the GRAS (GNSS Receiver for Atmospheric Sounding) sensor on-board the MetOp (Meteorological Operational) satellite (e.g., Loiselet et al. 2000) a fully operational system delivering RO observations will be available from 2006 onwards. On the other hand, the development of NWP systems during the last years improved the forecast skill and the quality of the analyses continuously. Thus it would be interesting to use the same methodology as used by NWP, to introduce data into the model (in our case via 3D-Var), first working with single sets of observations, later with whole climatologies, in order to study the increments of monthly and seasonal mean fields.

2 3D-Var System Implementation

2.1 Coordinate System

A GCM (Global Circulation Model) compliant Gaussian grid corresponding to T42L60, i.e., 64 latitude \times 128 longitude grid points, comprising 60 vertical model levels is used. The vertical coordinate system is based on the hybrid pressure coordinate provided by ECMWF analysis fields. From this basic vertical coordinate system, grids of geopotential height and geometric height (over reference ellipsoid) can be derived. The assimilation scheme can be used either with geometric height or geopotential height.

2.2 N and TQP_{surf} Analysis

The whole system can be run in two different modes. The first one performs a refractivity analysis (N analysis scheme), which means that refractivity observations are assimilated into a refractivity background. This background field is derived from ECMWF temperatures, specific humidity, and surface pressure fields using basically the same operators, which are used in the TQP_{surf} version of the assimilation scheme. This operation is performed at the beginning of the procedure, during the assimilation itself only the interpolation operators are used. The TQP_{surf} version of the assimilation scheme directly updates the temperature, specific humidity, and surface pressure background fields, which means that all fields are interpolated separately. At each successful iteration, the new pressure field has to be derived from the updated surface pressure field, and the refractivity has to be calculated at the location of the observation. After comparison of background refractivity (also denoted as model observation) and observation, the gradients of the input fields and observations are calculated and a suitable correction is applied.

2.3 Incremental 3D-Var

The solution of the minimization problem can be performed either in terms of full cost function fields $J(\mathbf{x}_a)$ or in terms of an analysis of increments

$$J(\mathbf{x}_a) = J(\mathbf{x}'_a = \mathbf{x}_a - \mathbf{x}_b), \quad (1)$$

where \mathbf{x}_a and \mathbf{x}_b are the analysis and the background state, respectively, and the prime superscript denotes the (1st order) increment. We chose the latter solution method, which provides optimal analysis increments, which are added to the unmodified background field. This procedure has a number of advantages like the use of linearized control variable transforms, which allow the straightforward use of adjoints to calculate the gradient of the cost function. Another advantage is that any imbalance introduced through the analysis procedure is limited to the small increments, which are added to the balanced first guess.

2.4 Control Variables

The control variables used in the analysis are temperature, specific humidity, and surface pressure, or refractivity transformed to logarithmic (LOG) space, to get a better conditioned problem, within the refractivity-only assimilation framework. In order to avoid negative specific humidities in the analysis and to get a better conditioned problem, the specific humidity is also transformed to and analyzed in LOG space. The cross correlations between the control variables are assumed to be small enough to be neglected. This assumption serves to effectively block-diagonalize the background error covariance matrix. For each control variable there still remains both, horizontal and vertical correlations. Those are assumed to be separable, which is a reasonable and widely used assumption.

Control Space Transformations

For a model state \mathbf{x} with n degrees of freedom, minimization of the cost function requires $O(n^2)$ calculations (Bouttier and Courtier 1999), thus becoming prohibitively expensive for usual n 's. One practical solution to this problem is to perform the minimization in a control variable space \mathbf{v} given by

$$\mathbf{x} = \mathbf{U}\mathbf{v}. \quad (2)$$

The transform \mathbf{U} has to be chosen in a way that

$$\mathbf{B} = \mathbf{U}\mathbf{U}^T \quad (3)$$

is approximately satisfied. In the control space \mathbf{v} the number of required minimization calculations is reduced from $O(n^2)$ to $O(n)$. Furthermore, by using the transform Eq. (3), the background error covariance matrix becomes

$$\mathbf{B}_v = \mathbf{I}, \quad (4)$$

hence effectively preconditioning the problem. \mathbf{I} denotes the identity matrix, \mathbf{B}_v the vertical background error covariance matrix. In terms of increments, the control variable transform can be written as

$$\mathbf{x}' = \mathbf{U}\mathbf{v}. \quad (5)$$

The inverse transformation

$$\mathbf{v} = \mathbf{U}^{-1}\mathbf{x}' \quad (6)$$

can be specified in different ways. The definition must provide a way to break down the atmospheric state \mathbf{x} into uncorrelated but physically realistic error modes, which can be penalized in J_b according to their estimated error magnitude (Barker 1999). See Löscher (2004) for more details.

Recursive-Filter Representation of Background Error Covariances

The control variable transform uses the identity $\mathbf{B}\mathbf{B}^T$ to define a transform $\mathbf{x}' = \mathbf{U}\mathbf{v}$, which relates preconditioned control variables \mathbf{v} to analysis increments in \mathbf{x}' in model space. The horizontal component \mathbf{U}_h , defined by

$$\mathbf{B}_h = \mathbf{U}_h \mathbf{U}_h^T, \quad (7)$$

is realized by scaled recursive filters (RF). The RF has to be applied in a non-dimensional space (e.g., Lorenc 1992).

2.5 Minimization

The cost function is minimized by using an iterative descent algorithm, which is in our case the L-BFGS-B routine, a quasi-Newton method. The cost of the analysis is proportional to the number of cost function and its gradient evaluations, denoted as simulations. If a new state \mathbf{x} is found, an iteration is performed, which means that to find a new \mathbf{x} , several simulations may be required. See, e.g., Byrd et al. (1994) for details.

2.6 Observation Operators

Horizontal Interpolation

The bi-linear interpolation consists of a weighted average of the four surrounding grid points to determine their interpolated value. Two linear interpolations on opposite sites are performed followed by a consecutive interpolation of these intermediate results. This horizontal interpolation is performed for the atmospheric layer above and below any given observation point.

Vertical Interpolation

Due to the fact of a globally non-uniform vertical grid, the heights of the horizontally interpolated values are also calculated by bi-linear interpolation from the vertical background grid. Given the interpolated background values above and below the spatial location of a given observation, a logarithmic vertical interpolation is finally performed to get the value of the background at the location of the observation. Generally interpolation needs great care to ensure negligible residual interpolation errors.

Vertical Coordinate Operator

The location of the observation is needed to calculate the refractivity. ECMWF provides temperature, specific humidity, and surface pressure fields. The background pressure field is derived by a series of operators. These operators are also

used to set up the vertical coordinate system of the assimilation scheme either as a vertical grid of geopotential heights or a vertical grid of geometric heights, respectively. Since the pressure field is also derived, pressure coordinates are possible as well but not implemented at the moment. The values of $T_{i,j,k}$ and specific humidity $q_{i,j,k}$ are given for the Gaussian grid of the latitudes φ_j and the homogenous grid of the longitudes λ_i , and an irregularly spaced height grid $z_{i,j,k}$. For the T42L60 grid, the index ranges are $I = 1 \dots 64$, $j = 1 \dots 128$, and $k = 1 \dots 60$ for full level quantities and $k = 0 \dots 60$ for half level quantities. The pressures corresponding to the k th half and full levels are calculated by the means of standard formulae (e.g., Roeckner et al. 2003). The calculation of the geopotential heights is based on the hydrostatic equation and on an interpolation between the half and the full levels (Gorbunov and Kornblueh 2003). The geometrical heights over reference ellipsoid are calculated from the geopotential heights by the approximate formula of the US Standard Atmosphere (Gorbunov and Kornblueh 2003).

Refractivity Operator

To calculate the refractivity N at any point, it is required to know the variables temperature T [K], specific humidity q or water vapor pressure e [hPa], and pressure p [hPa] or dry air pressure p_A [hPa]. There are two standard formulae used, the Thayer and Smith-Weintraub formulae (e.g., cited in Kursinski et al. 1997). The Thayer formula is slightly more accurate, the Smith-Weintraub formula is basically the same but assumes an ideal gas (compressibility factors $Z_{A,W}$ neglected). k_1, k_2, k_3 are the refractivity formula constants (e.g., Kursinski et al. 1997).

Thayer formula:

$$N = k_1 \frac{p_A}{T} \frac{1}{Z_A} + k_2 \frac{e}{T} \frac{1}{Z_W} + k_3 \frac{e}{T^2} \frac{1}{Z_W}. \quad (8)$$

Smith-Weintraub (3 terms) formula:

$$N = k_1 \frac{p_A}{T} + k_2 \frac{e}{T} + k_3 \frac{e}{T^2}. \quad (9)$$

2.7 Calculation of Refractivity Fields from ECMWF Analyses

Given the fields of temperature, specific humidity, and surface pressure (in our case analysis fields of ECMWF), we can calculate the field of refractivity using either the Thayer or Smith-Weintraub formula. A comparison of the two formulae shows no significant differences, which is also true when compared with CHAMP refractivity data, but because of negligible additional computing cost, the more accurate Thayer formula was chosen to calculate the background in the case of pure refractivity assimilation, and as forward operator to calculate refractivity from temperature, humidity, and surface pressure fields. To derive the error characteris-

tics in case of the pure refractivity assimilation scheme, the Smith-Weintraub formula was used.

3 Error Formulation

3.1 Observation Error Covariance

The observation error covariance only takes vertical correlations into account. Due to the separation in space and time between the different RO events (mean distances generally >300 km, time differences >1.5 hrs) this simplification is justified.

Formulation of the Observation Error Covariance Matrix

A simple error covariance matrix formulation was deduced from the empirical estimated matrices following Steiner and Kirchengast (2005). A least-squares method was used to fit analytical functions to the relative standard deviation, which shows a different behavior below and above the tropopause height z_{Tropo} . The empirical relative standard deviation S_z can be approximated with an exponential increase above z_{Tropo} , Eq. (10), and with a decrease proportional to $(1/z)$ below z_{Tropo} , Eq. (11). z_{Tropo} is defined here globally at 15 km; simplified from Steiner and Kirchengast (2005) no constant error range around 15 km is used in this study. To be able to scale the error magnitude, which is receiver dependent, the tropopause standard deviation s_{Tropo} can be tuned, we used 0.4 % based on experience with CHAMP data. Eq. (10) gives the exponential function for the relative standard deviation above z_{Tropo} , with the parameter H_{Strato} , which is the scale height of the error increase over the stratosphere. The value for global H_{Strato} was set to 11.9 km for the error scale height (Steiner and Kirchengast 2005).

$$S_z = s_{\text{Tropo}} \exp[(z - z_{\text{Tropo}}) / H_{\text{Strato}}], z \geq z_{\text{Tropo}} \quad (10)$$

Eq. (11) gives the analytical function for the relative standard deviation below z_{Tropo} , where the near-surface ($z \sim 1$ km) error $s_0 = 4.46$ %.

$$S_z = s_{\text{Tropo}} + s_0 (z^{-1} - z_{\text{Tropo}}^{-1}), z < z_{\text{Tropo}} \quad (11)$$

This formulation of the observation error covariance also accounts for the error of representativeness, thus no additional specification of this is necessary within the assimilation framework. A somewhat improved representation of the observation error is presented by Steiner et al. (2006), based on a CHAMP data error analysis.

3.2 Background Error Covariance

The used background fields of temperature, specific humidity, and surface pressure were provided by ECMWF. Thus the basis of our considerations concerning the background errors and their correlations are based on ECMWF recommendations (M. Fisher, ECMWF Reading, UK, pers. communications, 2003). For the refractivity assimilation scheme, the error characteristics have been derived using error propagation techniques. The relative standard deviation ranges from $\sim 1.5\%$ at the surface to $\sim 0.8\%$ at the uppermost levels with a peak of $\sim 2.8\%$ within the troposphere; see Löscher (2004) for details.

4 First Results

Among a large number of smaller simulation experiments (Löscher 2004), a quasi-operational run was performed for the “testbed month” August 2003. The complete August 2003 was processed day-by-day, dividing each day into four assimilation windows of 6 hours per day, using the corresponding ECMWF analyses as first guess. This translates into 31 independent time slices, around 00 UTC, 06 UTC, 12 UTC, and 18 UTC, delivering 124 analyses over the month. The global quite even distribution of the 4482 CHAMP RO profiles (about 150 profiles per day) of August 2003 (see Fig. 1), comprises 245 220 single observational values.

A lower cut-off height of 5 km was chosen, based on other studies suggesting that the CHAMP data quality degrades rapidly below 5 km. This problem has to be solved at retrieval level by advanced wave optics methods (e.g., Jensen et al. 2003) to enable effective use of observations below 5 km. The analysis fields were averaged separately for each time layer of each day and in addition a total monthly mean was derived by averaging the time layer means. These averaged fields were compared to the corresponding monthly mean analysis fields of ECMWF. This procedure was applied for the refractivity and the temperature, specific humidity, and surface pressure assimilation schemes. The minimization process was stopped after 20 cost function and gradient evaluations (a number based on extensive sensitivity and convergence tests), leaving some safety margin, which practically meant that about 5 to 6 successful iterations were found sufficient for completing the analysis within each assimilation time window. The comparison between the two assimilation schemes (N and TQP_{surf}), agrees well, especially above the troposphere.

As an alternative approach concerning the choice of the ECMWF background fields, short-range (24 hr and 30 hr) forecasts and the corresponding error characteristics will be used in future. This will be a better choice of background data for climate monitoring applications and climate studies, since the short-term forecasts will provide physically consistent atmospheric states independent of details of the initial condition analysis, which in future will presumably have assimilated radio occultation data itself routinely via ECMWF’s analysis and prediction system

(Healy and Thépaut 2005). Another possible approach might be the derivation of first guess fields from reanalysis projects like ERA40 (ECMWF 40 year Reanalysis), taking a time frame of the last 20 years into account.

As an example of the preliminary assimilation results (see Fig. 2), the increment of the total refractivity assimilation (mean of all time layers) for August 2003 for a model level near 20 km height is shown. It can be seen that any non-persistent deviations are vanishing within the monthly mean delivering a neutral result, leaving only a significant increment over the southern high latitudes. As the RO observations are an independent source of information, these results indicate a systematic deviation within certain regions of the ECMWF analysis fields. A bias within the RO refractivities themselves cannot currently be excluded from the considerations (we applied a 0.4 % correction prior to the assimilation experiments); cf., the error analysis results of Steiner et al. (2006); improved retrieval algorithms are expected to solve this problem. On the other hand, a systematic deviation introduced by the observations would be expected to be globally evenly distributed (see Fig. 1). This not being the case, strengthens evidence of a systematic deviation within certain regions of the ECMWF background data. This evidence is roughly consistent with the significantly more elaborated inter-comparison of seasonal mean RO-only climatologies of dry temperature and refractivity with the corresponding ECMWF fields (Gobiet et al. 2005; Borsche et al. 2006). Next steps of the work are further advancement of the assimilation scheme and larger-scale application to longer radio occultation datasets, using ECMWF short-range forecasts as background.

5 Conclusion

The first results are promising and show that the information content of RO data is not redundant, thus the observations introduce useful information in ECMWF analysis fields. Furthermore, these findings suggest that the operational use of RO data within NWP frameworks yields a promising perspective for the future (see also Healy and Thépaut 2005). In that respect especially the stratospheric temperature information seems to have a significant impact. A variational climate monitoring framework based on RO data will provide the opportunity to study increments over time, and gain insight into the characteristics of the used background fields. First-guess fields from re-analysis data might be another interesting background option in the future, to be independent from operational model updates.

Acknowledgments: The authors are grateful to A.K. Steiner (WegCenter, Univ of Graz, Austria) for valuable inputs regarding the observation error characteristics as well as to M. Fisher (ECMWF, Reading, UK) for supplying background error covariances. The authors also gratefully acknowledge T. Schmidt, J. Wickert and the full team at GFZ Potsdam, Germany, for the provision of CHAMP data and A. Gobiet and M. Borsche (WegCenter, Univ of Graz, Austria) for related refractivity retrieval processing. A.L. was funded from the START research award of G.K. financed by the Austrian Ministry for Education, Science, and Culture and managed under Program Y103-N03 of the Austrian Science Fund.

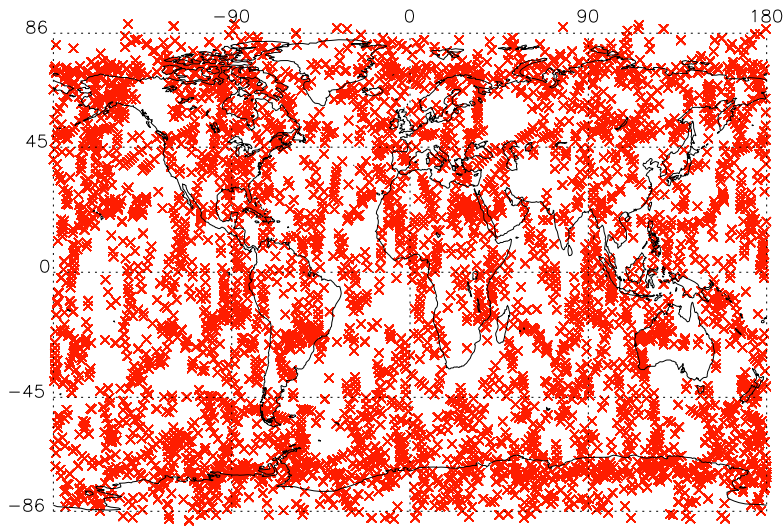


Fig. 1. Geographic distribution (longitude vs. latitude map) of the 4482 occultation profiles used within the assimilation experiment covering August 2003.

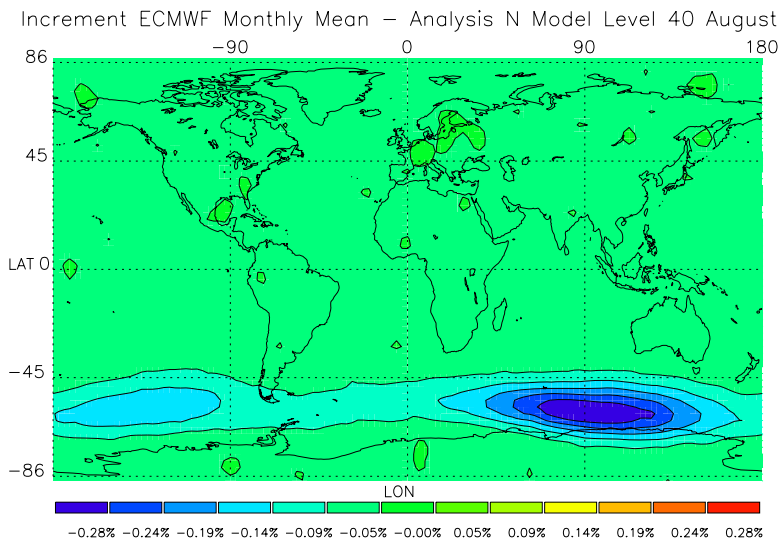


Fig. 2. Increment of the refractivity assimilation of August 2003 between analysis and ECMWF background (monthly mean of all time layers) in a longitude-latitude map for model level 40 ($z \sim 20$ km).

References

- Barker D (1999) A general formulation for 3D-Var control variables. Part of the WRF package (also available on request from the first author, A.L.)
- Borsche M, Gobiet A, Steiner AK, Foelsche U, Kirchengast G, Schmidt T, Wickert J (2006) Pre-Operational retrieval of radio occultation based climatologies. This issue
- Bouttier F, Courtier P (1999) Data assimilation concepts and methods. Meteorological Training Course Lecture Series, ECMWF Reading, UK
- Byrd RH, Peihuang L, Nocedal J, Zhu C (1994) A limited memory algorithm for bound constrained optimization. Tech Rep NAM-08, Northwestern University, USA
- Gobiet A, Foelsche U, Steiner AK, Borsche M, Kirchengast G, Wickert J (2005) Climatological validation of stratospheric temperatures in ECMWF operational analyses with CHAMP radio occultation data. *Geophys Res Lett* 32(L12806), doi:10.1029/2005GL022617
- Gorbunov ME and Kornblueh L (2003) Principles of variational assimilation of GNSS radio occultation data. Tech Rep No 350, MPI for Meteorology, Hamburg
- Jensen AS, Lohmann M, Benzon H-H, Nielsen A (2003) Full spectrum inversion of radio occultation signals. *Radio Sci* 38(3), doi:10.1029/2002RS002763
- Healy SB, Thépaut JN (2005) Assimilation experiments with CHAMP GPS radio occultation measurements. *Q J R Meteorol Soc*, in press
- Kursinski, ER, Hajj GA, Schofield JT, Linfield RP, Hardy KR (1997) Observing earth's atmosphere with radio occultation measurements using the Global Positioning System. *J Geophys Res* 102:23429–23465
- Löscher A (2004) Assimilation of GNSS radio occultation data into GCM fields for global climate analysis. Wissenschaftl Ber No 22, IGAM, Univ of Graz, Austria
- Loiselet M, Stricker N, Menard Y, Luntama J-P (2000) GRAS –Metop's GPS-based atmospheric sounder. *ESA Bulletin* 102:38–44
- Lorenz AC (1992) Analysis methods for Numerical Weather Prediction. *Q J R Meteorol Soc* 112:1177–1194
- Roeckner E et al. (2003) The atmospheric general circulation model ECHAM5, Part I: Model description. Tech Rep No 349, MPI for Meteorology, Hamburg
- Steiner AK, Kirchengast G (2005) Error analysis for GNSS radio occultation data based on ensembles of profiles from end-to-end simulations. *J Geophys Res* 110(D15307), doi:10.1029/2004JD005251
- Steiner AK, Löscher A, Kirchengast G (2006) Error characteristics of refractivity profiles retrieved from CHAMP radio occultation data. This issue
- Wickert J, Galas R, Schmidt T, Beyerle G, Reigber C, Foerste C, Ramatschi M (2004) Atmospheric Sounding with CHAMP: GPS ground station data for occultation processing. *Phys Chem Earth* 29:267–275